

Research Article

Research on Structural Characteristics of Dynamic Nuclear Zone in Dynamic System of Coal and Rock

Hai Rong ^{1,2}, Bing Liang,² Hongwei Zhang ¹ and Feng Zhu¹

¹College of Mining, Liaoning Technical University, Fuxin, Liaoning Province, China

²School of Mechanics and Engineering, Liaoning Technical University, Fuxin, Liaoning Province, China

Correspondence should be addressed to Hai Rong; ronghai1988@163.com

Received 21 October 2018; Accepted 20 February 2019; Published 12 March 2019

Academic Editor: Eric Lui

Copyright © 2019 Hai Rong et al. This is an open access article distributed under the Creative Commons Attribution License, which permits unrestricted use, distribution, and reproduction in any medium, provided the original work is properly cited.

In order to calculate the concrete scale range of coal and rock mass in rockburst of different degrees of danger and to prevent and control rockburst in coal mines, the concept of dynamic system of coal and rock is put forward in this paper. The model of the relationship between the occurrence of rockburst and dynamic system is built at the same time, which could be used to analyze the rockburst risk of coal and rock in different scales. The calculation method of dynamic nuclear zone scale and its evaluation system and quantitative indicators are put forward based on the energy release process of dynamic system of coal and rock. Combined with the fracturing technology of liquid CO₂, the accuracy of the calculation method for the radius of dynamic nuclear zone is verified in a coal mine in Shanxi Province. The degree of coincidence between the results of the two methods is 96.9%~97.5%, which shows that the calculation method for the radius of dynamic nuclear zone has high reliability and practicability. This method can be widely used in forecasting the risk of rockburst. The liquid CO₂ fracturing method can be well used to simulate the blasting source of rockburst at the same time and can be applied to more mines in the future.

1. Introduction

The shallow coal resources account for 47% of the total coal reserves in China which have been nearly exhausted after a long period of mining [1]. At the International Coal Summit 2013 held in Beijing, China, Xie, an academician of the Chinese Academy of Engineering predicted that China's total coal annual output will reach 3 to 3.5 billion tons by 2030, and this output level will continue for several years to come [1]. It means that in order to meet China's annual demand for coal resources, more coal mines in China will reach the "deep mining" level in the near future. Coal and rock will bear higher stress and energy when the coal mine reaches the "deep mining" level, providing a more conducive environment for the occurrence of rockburst [2–5]. Rockburst is one of the most common and destructive mine dynamic disasters, which poses a serious threat to the safety of coal mine workers and the efficient production of coal mines [6]. Therefore, accurate evaluation and prediction is particularly important for the establishment of mine rockburst prevention and control systems.

Many theories and methods have been formulated for the evaluation and prediction of coal mine impact pressure, and good application results have been obtained in many mines. In order to identify the information that can be used to predict dynamic disasters, Vazaios et al. [7] investigated the failure and fracturing processes and the mechanisms of energy storage and rapid release resulting in rockbursting by finite-discrete element method and examined the impact of rock structure on rockbursting under high in situ stresses by integrating DFN geometries. Wang et al. [8] regarded the rock strength index, energy release index, and surrounding rock stress as the basic factors of rockburst, and a new Bayesian multi-index model to predict and evaluate rockbursts was built, which was observed to predict rockbursts more effectively than the current methods. Wang and Kaunda [9] indicated that the rockburst consequence could be quantified with plastic strain work and released energy in numerical models, and they thought the rock mass damage under soft loading stiffness had larger magnitude of plastic strain work and released energy than that under stiff loading stiffness. Sousa et al. [10] focused on the analysis of

a database of in situ cases of rockburst, the in situ rockburst database was further analyzed using different DM techniques ranging from ANNs to naive Bayesian classifiers in order to build influence diagrams, list the factors that interact in the occurrence of rockburst, and understand the relationships between these factors. Zhang et al. [11] revealed the power sources and energy accumulation conditions of rockburst under natural geological conditions by applying the geodynamic division method and predicted the dangerous locations of rockburst in the Shenhua Xinjiang mining area in China. Pan et al. [12, 13] proposed the charge induction monitoring theory and developed a working charge induction monitoring system. Experiments have shown the system is accurate in monitoring the spatial and temporal changes of the coal surface charge with a range of applied stress during the mining process. Dou et al. [14] analyzed the theoretical basis of the seismic tomography to detect and evaluate the impact risk and determined the index and critical value of the seismic tomography detection technology, based on the experimental relation model between longitudinal wave velocity and stress. Jiang et al. [2] studied the relationship and difference between rockburst, rock blasting, and mine earthquake and proposed 3 mechanical models of rockburst in coal mine. They identified 4 categories of scientific problems that need to be addressed in the study of rockburst and pointed out the direction of improving the level of rockburst prevention and control. Jiang et al. [15] put forward a method based on the stress superposition to assess rockburst risk after fully considering the influence of various factors on the increment of the geostatic stress. He considered this method more intuitive and quantified for the evaluation of rockburst. Pan et al. [16] aimed to identify the inducing factors of rockburst in their research. They proposed the theory of the source monitoring and evaluation and established the evaluation model based on weight comprehensive and different-load sources of coal bump. The authors believed that the method can effectively reflect the current degree of risk and the future development trend of rockburst. The weight is calculated according to the contribution rate of coal bump monitoring index by the entropy weight method that could reduce the influence of subjective factors. Based on the impact tendency of coal, Li et al. [17] studied the relevant information before the damage of coal and revealed the fact that the amplitude of the main frequency of acoustic emission increases with the increase of coal impact tendency and the stress value of coal is negatively correlated with the acoustic emission signal “b.” The “hierarchical monitoring application” model of rockburst was established by Lv et al. [18] He applied the model to the Xinzhouyao coal mine, Datong mining area, and believed that the complementarity between the hierarchical monitoring technology and other monitoring technologies is strong. The technology can enable effective comprehensive dynamic monitoring of the mine. Peng et al. [19] established the rockburst risk preevaluation index based on the corresponding influence factors, constructed the dynamic preevaluation system and verified the rationality of the system in practice.

When the structure of coal and rock is destroyed, the accumulated energy will be released in the form of waves,

which will be accompanied by microseismic signals [20]. The occurrence of rockburst is the unity of time and space. Since there is often a high-energy microseismic event in the process of rockburst, the accurate prediction of the high-energy microseismic event is the key to rockburst prediction [19]. Therefore, the analysis of microseismic events should be focused on their locations and energy, especially “high-energy” microseismic events above the critical energy of rockbursts.

When a high-energy microseismic event occurs, there is greater potential danger of damage to the coal and rock nearby [21]. After a period of energy accumulation, the coal and rock mass in the nearby areas are in danger of rockburst or high-energy microseismic events occurring again. According to statistical analysis, 10^6 J is regarded as the critical energy of rockburst in China. We should focus on the microseismic events above the critical energy of rockburst for each mine with rockburst danger.

2. Model Construction and Energy Source for Dynamic System of Coal and Rock

2.1. Concept and Model Construction for Dynamic System of Coal and Rock. Different geological dynamic environments have been formed due to tectonic movements, which resulted in different stress distribution and energy accumulation of rock mass. When the mining activity reaches a zone of high stress or energy accumulation, the risk of coal and rock structure instability, energy release, rockburst, and other mine dynamic disasters is increased. We define the coal and rock system in this zone as “dynamic system of coal and rock,” and the basic power source of rockburst is the energy released from dynamic system of coal and rock. In the dynamic system of coal and rock, there are many factors that affect its stability, of which energy factor is the most important. Determining the source and scale of the dynamic system of coal and rock will be helpful to the prediction and prevention of rockburst.

The occurrence of rockburst originates from the difference between the released energy and absorbed energy when the coal and rock are destroyed, reaching or exceeding a certain critical value. The difference in energy depends on the relative spatial relationship between mining work and dynamic system of coal and rock, which leads to the different dynamic appearance of rockburst. We constructed the model of the relationship between rockburst and dynamic system of coal and rock and formulated the corresponding relationship criteria, as shown in Figure 1.

According to the degree of energy accumulation and the influence range, dynamic system of coal and rock can be divided into four zones: the dynamic nuclear zone, the damage zone, the injury zone and the influence zone. Rockburst can also be categorised into four grades: coal gun, coal pour out or press out, rockburst and serious rockburst. When mining activity reaches the influence range, injury zone, damage zone and dynamic nuclear zone, the corresponding dynamic behavior will be coal gun, coal pour out or press out, rockburst and serious rockburst respectively.

Therefore, to prevent and control rockburst, it is important for us to study the structure of dynamic system of coal and rock and determine the calculation method of each

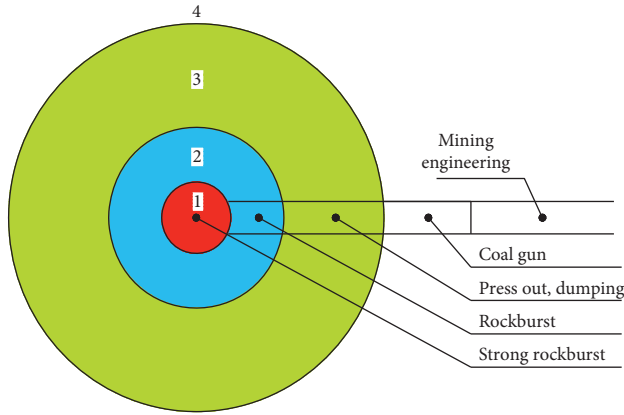


FIGURE 1: Model of the relationship between rockburst and dynamic system of coal and rock: (1) dynamic nuclear zone; (2) damage zone; (3) injury zone; (4) influence zone.

regional scale for rockburst. In particular, to determine the scale radius of dynamic nuclear zone is the basis of studying the structure of dynamic system of coal and rock and the foundation of determining the danger of rockburst. In this paper, our research mainly focuses on the scale radius of the dynamic nuclear zone.

2.2. Energy Source of Dynamic System of Coal and Rock. The release of energy is a necessary condition for all kinds of geological dynamic disasters and mine dynamic disasters. Generation of energy is caused by the deformation of materials. Because of the difference in geological medium

material, movement velocity and extrusion degree of tectonics are different, and the ability of energy transfer and storage in geological bodies is also different. Natural geological condition and mining effect are the two sources that the energy of dynamic system of coal and rock comes from. Dynamic system of coal and rock located in the tectonic environment and the modern stress field, with dynamic conditions for forming energy accumulation. Through the work such as mining and excavation, the stress of the system will be increasing, the energy will be superimposing, and the system will maintain dynamic equilibrium. At the same time, mining activities will change the energy of the dynamic system, release energy into the system, destroy the structure of the system, and cause dynamic disasters such as dynamic emergence or rockburst.

Total energy of dynamic system is made up of energy under gravity stress field U_Z , energy under tectonic stress field U_G , and energy under mining induced stress field U_C , as shown in formulas (1)–(4) [22]. In this paper, dynamic system is regarded as a spheroid, which the scale radius is R , and the volume is V , as shown in formula (5). The scale of dynamic system is related to the stored energy and the released energy. Therefore, the actual scale of dynamic system can be determined according to the energy value of rockburst and “high-energy” microseismic events. In this paper, the radius of the dynamic nuclear zone, the damage zone, the injury zone, and the influence zone are expressed by R , R_p , R_s , and R_Y respectively. The three-dimensional model of dynamic system of coal and rock is shown in Figure 2.

$$U = U_Z + U_G + U_C, \quad (1)$$

$$U_Z = \frac{\int_{i=1}^{i=n} [\gamma_i^2 H_i^2 + 2(\mu^2 / (1 - \mu)^2) \gamma_i^2 H_i^2 - 2\mu(2(\mu / (1 - \mu)) \gamma_i^2 H_i^2 + (\mu^2 / (1 - \mu)^2) \gamma_i^2 H_i^2)]}{2E_i}, \quad (2)$$

$$U_G = \frac{\int_{i=1}^{i=n} [(k_1^2 + k_2^2 + k_3^2) \gamma_i^2 H_i^2 - 2\mu(k_1 k_2 + k_2 k_3 + k_1 k_3) \gamma_i^2 H_i^2]}{2E_i}, \quad (3)$$

$$U_C = (1 + m_1)U_Z + (1 + m_2)U_G, \quad (4)$$

$$V = \frac{4}{3} \pi R^3. \quad (5)$$

Under the influence of external forces such as tectonic movements and mining activities, the coal and rock in the mine will deform, and the deformation of the coal and rock will be accompanied by the continuous accumulation of energy. Once the external force on the coal and rock disappears, the accumulated energy in the coal and rock will be

released while the coal and rock restores its original shape [23, 24].

When rockburst is absent, dynamic system of coal and rock continuously accumulates energy. Under the influence of mining disturbance, when the total energy of dynamic system is greater than the background energy, the energy will be released. If the released energy ΔU is greater than the critical energy, the rockburst will occur.

(1) Energy under gravity stress field

Under the gravity stress field, the energy stored in dynamic system is related to the mining depth. With the increase of the mining depth, the weight of overlying strata increases, and the energy stored in the system increases.

(2) Energy under tectonic stress field

The energy stored in rock is related to the elastic deformation of the rock mass, and the greater the elastic deformation, the more the energy stored. Dynamic system of coal and rock under tectonic

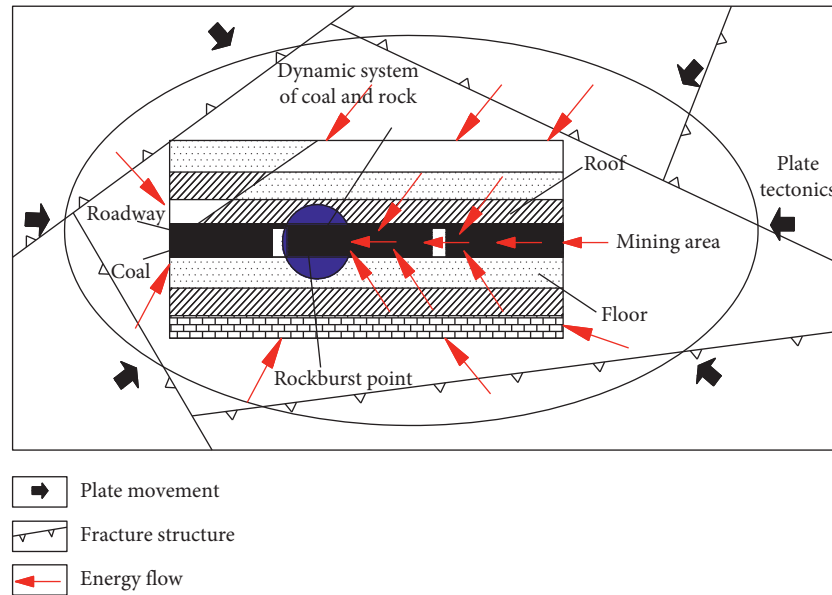


FIGURE 2: Energy sources of coal dynamic system.

stress field is also experiencing elastic deformation; dynamic system accumulates energy with the increase of elastic deformation. When the stress reaches the ultimate strength of the rock, the rock will be destroyed. For dynamic system of coal and rock, this part of energy is produced by the combined action of gravity stress field energy and tectonic stress field energy. The energy released from dynamic system of coal and rock is equal to the energy difference between tectonic stress field and gravity stress field, as shown in the following equation:

$$\Delta U = U_G - U_Z. \quad (6)$$

(3) Energy under mining induced stress field

Due to the influence of mining engineering, the stress state of coal and rock will change, and the energy of dynamic system will also change accordingly. Because of difference in mining areas, mines, coal seams, structures, and stress conditions, the mode of rockburst is different. Therefore, m_1 and m_2 should be confirmed by theoretical calculation, numerical calculation, analogue material simulation, etc.

3. Calculation for the Scale of Dynamic Nuclear Zone

3.1. Analysis of Dynamic Nuclear Zone Formation Process. The energy of dynamic system is mainly concentrated in the “dynamic nuclear zone.” Similar to the unloading blasting process of coal, at the instance when rockburst or high-energy microseismic event occurs, the “dynamic nuclear zone” of dynamic system will form a huge impact load, which satisfies the von Mises yield criterion. Under the action of the impact load, the outer wall of the “dynamic nuclear zone” of dynamic

system is deformed rapidly. The coal and rock mass at the junction of the “dynamic nuclear zone” and the “destroyed area” will generate a shock wave rapidly, which immediately propagates and dissipates to the outer region. In this process, the coal and rock in the “dynamic nuclear zone” is completely broken, as shown in Figure 3. Under the action of the shock wave, the coal and rock mass in a certain range outside the “dynamic nuclear zone” will receive the compressive stress far greater than the dynamic compressive strength of the coal and rock themselves. In this process, the coal and rock in this section will break up under the strong compressive stress, forming a “ring damage zone.” The “damage zone” of dynamic system is formed outside the “dynamic nuclear zone,” as shown in Figure 4.

In the “damage zone” of dynamic system, shock wave is the main form of energy and the strength of which is far greater than the dynamic compressive strength of coal and rock, as shown in Figure 5. Compression failure will occur in coal and rock, the failure criterion of coal in this section is based on the dynamic compressive strength of coal itself, and the boundary condition is that shock wave strength is equal to the dynamic compressive strength of coal itself.

3.2. Calculation of Dynamic Nuclear Zone Radius of Coal Rock Dynamic System. The energy of dynamic system is mainly concentrated in the “dynamic nuclear zone.” The energy released when rockburst or high-energy microseismic events are monitored by microseismic system and other equipment is provided by the “dynamic nuclear zone” of dynamic system. Under the influence of geological dynamic conditions, the energy of dynamic system mainly comes from tectonic stress field. After the energy transfer and supplement between dynamic system and the outside world, the dynamic system maintains a balanced state. After a rockburst accident occurs, there is still some residual energy in

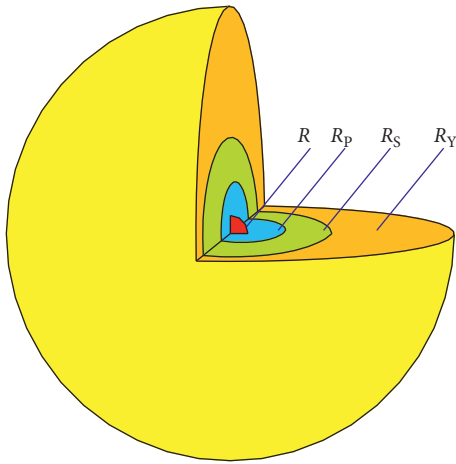


FIGURE 3: Dynamic system stereomodel of coal and rock.

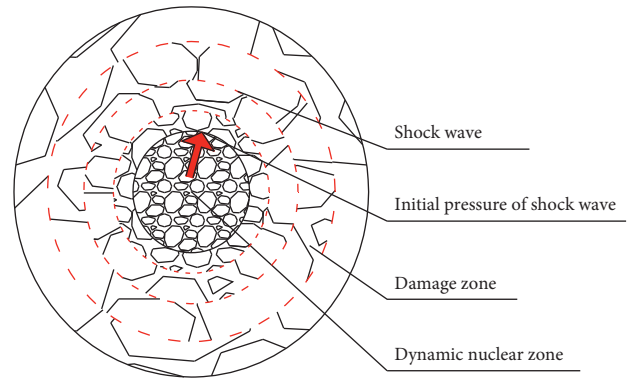


FIGURE 5: Damage zone formation process.

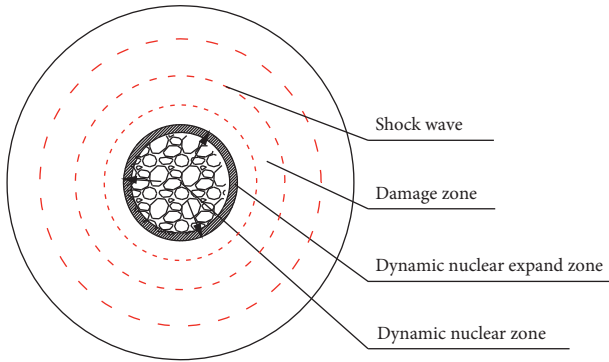


FIGURE 4: Dynamic nuclear zone failure process.

the dynamic system. If the energy accumulated in the dynamic system is enough to support the next rockburst

accident, the rockburst will reoccur when induced by mining activities and other factors. The radius “R” of the “dynamic nuclear zone” of the dynamic system can be deduced and calculated according to formulas (2), (3), and (5)–(7) under the model conditions of the “spherical” dynamic system, as shown in formula (8).

The calculation method of radius “R” of “dynamic nuclear zone” in dynamic system needs to be verified by other experimental methods such as liquid CO₂ fracturing technology.

$$\Delta U = \frac{2\pi\gamma^2 H^2 R^3}{3E} \times \left[(k_1^2 + k_2^2 + k_3^2) - 2\mu(k_1k_2 + k_2k_3 + k_1k_3) - 1 + \frac{2u^2}{(1-\mu)} \right], \quad (7)$$

$$R = \sqrt[3]{\frac{3E(1-\mu)\Delta U}{2\pi[2\mu^2(k_1k_2 + k_1k_3 + k_2k_3 + 1) - \mu(2k_1k_2 + 2k_1k_3 + 2k_2k_3 + k_1^2 + k_2^2 + k_3^2 - 1) + k_1^2 + k_2^2 + k_3^2 - 1]\gamma^2 H^2}}. \quad (8)$$

4. Principle and Equipment of Liquid CO₂ Fracturing

4.1. Structure and Equipment of Liquid CO₂ Fracturing. CO₂ fracturing device is a new type of fracturing equipment for coal mining, which mainly comprises of a filling valve, a heating pipe, a main pipe, a sealing gasket, a shearing piece, and a discharge head. Structure and composition of CO₂ fracturing device are shown in Figure 6. The filling valves, the main manifolds, and the discharge heads are reusable, made of high-strength metals, whereas the heating pipes, the gaskets, and the shears are consumables. After taking a fracturing device filled with liquid CO₂ to the borehole, the heating pipe will be turned on by the initiator. The liquid CO₂ in the main pipe gasifies rapidly. The pressure in the main pipe builds up, until the pressure release mechanism

breaks the shear fragment, releasing a large volume of CO₂ gas to fracture the coal.

4.2. Mechanism of Liquid CO₂ Fracturing. Under standard temperature and pressure, CO₂ is a colorless, odorless, and noncombustible gas. When the temperature of liquid CO₂ exceeds 31.1°C while the pressure is held above 7.35 MPa, CO₂ enters the supercritical state. Above the critical temperature, the gaseous substance will remain in its original state and will not continue to liquefy, even if the pressure is higher. CO₂ in its supercritical state is neither gas nor liquid, but presents as a state between gas and liquid, and has the characteristics of both.

When the liquid CO₂ fracturing technology is applied, the fracturing only occurs in the interior of the medium, and there is no free surface in blasting. Most of the gas emitted by



FIGURE 6: Sketch map of composition structure of CO₂ fracturing device: (1) filling valve; (2) fever tube; (3) chief tube; (4) seal; (5) shear sheet; (6) spillage head.

the cracker will act in the normal direction of the borehole, which is based on the action of high pressure shock cracking from CO₂. We fill the main pipe of the fracturer with liquid CO₂ and use the initiator to excite the heating pipe quickly, and the liquid CO₂ gasifies and expands instantaneously and produces high pressure. When the pressure reaches the limit strength of the constant pressure of shear piece, the shear piece will be broken, and the high pressure gas is released from the discharge head and acts on the coal and rock to realize the directional fracturing, as shown in Figure 7.

We regard the destroyed area of coal as a part of a sphere. According to the minimum energy principle of rock dynamic failure [25], the minimum energy required for the failure of fractured coal mass is shown in formulas (9) and (10). The occurrence of rockburst or high-energy micro-seismic events will be accompanied by the transmission of shock waves and stress waves. After the dynamic nuclear zone of dynamic system is formed in the broken coal, the damage zone, injury zone, and influence zone of dynamic system will be formed, with the gradual attenuation of stress and the gradual dissipation of shock wave energy. The liquid CO₂ fracturing technology exploits the high-pressure impact released during the gasification process, and the dynamic nuclear zone of dynamic system is formed without shock waves. Therefore, the energy released by the liquid CO₂ fracturing equipment can be calculated by measuring the fracturing range of liquid CO₂ in coal. The amount of energy released can subsequently be used in the proposed radius calculation method of the dynamic nuclear zone. By comparing the calculation results and the experimental data, the accuracy of the method can be determined.

$$V_s = \frac{4}{3}\pi L^3 \times \frac{\theta}{2\pi} = \frac{2}{3}L^3\theta, \quad (9)$$

$$U_s = \frac{\sigma_c^2 V_s}{2E} = \frac{\sigma_c^2 L^3 \theta}{3E}. \quad (10)$$

5. Field Verification of Radius Calculation Method for Dynamic Nuclear Zone

5.1. Experimental Layout and Mechanical Parameters of Coal and Rock. We conducted an industrial test on coal pillar side of 5939 roadway, panel 8939, in a coal mine of Shanxi Province by using the ZLQ-53/800 CO₂ fracturing equipment. Its specifications are shown in Table 1. 9 holes with different diameters were drilled, with 3 at 60 mm, 3 at 65 mm, and 3 at 90 mm. According to the degree of coal failure and pressure relief effect, the optimal drilling diameter of CO₂ fracturing is obtained, and the accuracy of radius calculation method for dynamic nuclear zone of dynamic system is verified.

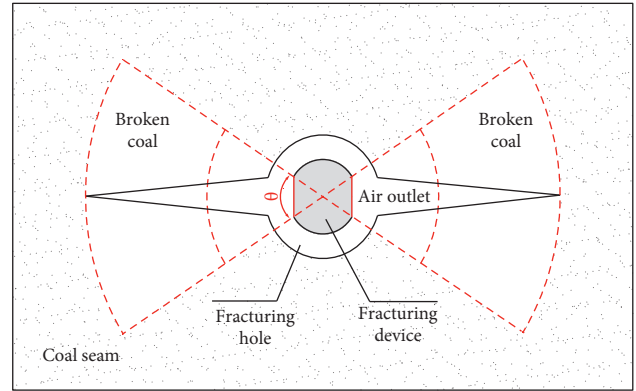


FIGURE 7: Schematic diagram of CO₂ fracturing device.

The measurement results of the physical and mechanical indexes of coal in panel 8939 are shown in Table 2. Current mining depth in this area is 340 m. The result of in situ stress test is 12.95 MPa (maximum principal stress), 7.29 MPa (intermediate principal stress), and 7.14 MPa (minimum principal stress).

5.2. Determination of Fracturing Effect Parameters. In order to determine the fracture range of liquid CO₂ in panel 8939, we relied on the distributed optical fiber sensing technology to monitor the fracturing effect and influence range. Fibers that carry optical signals are used to sense and transmit measurement results. It is immune to electromagnetic interference, highly sensitive, waterproof and moisture-proof, and capable of long-range and wide-area monitoring. The infrastructure is easy to install, has good material quality, and lasts for a long time. Distributed optical fiber sensing technology is based on Brillouin optical time-domain analysis technology, which can measure the strain of each point in the optical fiber in a distributed way to achieve precise, continuous, and universal monitoring, as shown in Figure 8.

After grouting and sealing, the distributed sensing fiber optic cables and the pressure testing tube are consolidated together with the surrounding coal body to coordinate deformation. We set liquid CO₂ fracturing hole under the fiber optic cable; when coal deformation occurs after pressure relief, fiber optic will sense the deformation of the test tube strain, and then calculate the pressure pipe stress distribution curve, according to the stress and strain coefficient of the pressure. Distributed sensing fiber optic cables arranged beside pressure pipes will bend and stretch under the action of surrounding coal. This stretching deformation area is the influence area of coal pressure relief deformation, as shown in Figure 9.

We set a distributed optical fiber monitoring hole at the winch hole location in roadway 5939 near the stopping line

TABLE 1: Specifications of liquid CO₂ fracturing instrument.

Model	External diameter (mm)	Internal diameter (mm)	Length of main pipe (mm)	Length of reel (mm)	Shear strength (MPa)	Gas loading (kg)
ZLQ53/800	53	37	800	250	300	0.530

TABLE 2: Physical and mechanical indexes of coal seam on panel 8939.

Lithology	Uniaxial tensile strength (MPa)	Uniaxial compressive strength (MPa)	Hardness	Modulus of elasticity (GPa)	Poisson ratio	Internal friction angle (°)	Cohesive force (MPa)
Coal	1.34	32.27	3.23	3.66	0.20	29.89	3.67

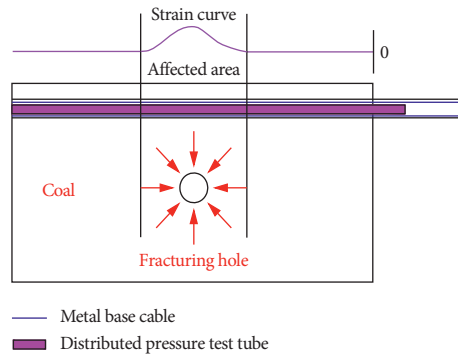


FIGURE 8: Test principle diagram of pressure relief influence range.

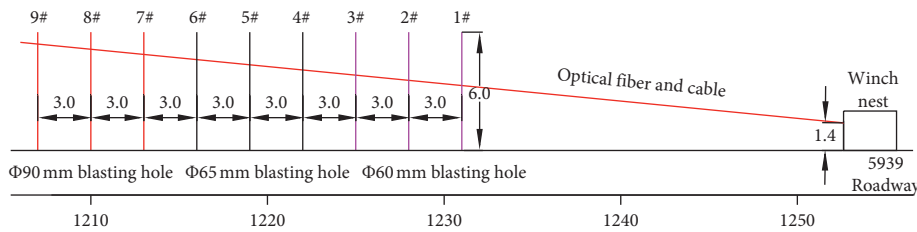


FIGURE 9: Borehole layout plan.

of panel 8939. The winch hole is 1.4 m away from the coal wall, 1.2 m away from the bottom plate. The angle between the optical fiber monitoring hole and the coal wall is 5 degrees. The hole has an elevation angle of 1 degree, a diameter of 65 mm, and a depth of 50 m.

After the completion of the optical fiber hole, we arranged a 50 m long distributed optical fiber sensing cable. Since the fiber optic cables are laid on an inclined surface, the construction is only carried out at 1207 m~1235 m on the panel for the safety of roadway. A total of 9 liquid CO₂ blasting holes were drilled in 20 cm below the fiber to analyze and monitor the effect of coal fracturing.

5.3. Analysis of Fracturing Effect. The strain of the sensing cable mainly reflects the deformation characteristics of the coal around the borehole along the radial direction of the fiber. Figure 10 shows the strain distribution curve of sensing cable in the monitoring hole. Generally, tensile strain is defined as a positive value and the compressive strain as a negative value. The cable is generally under tensile strain,

which indicates that the tension around the borehole occurs along the radial direction of the optical fiber.

The ZLQ53/800 type fracturer is used to construct a drilling hole with a diameter of 60 mm, the distance between the fracturer and the hole wall is 7 mm. The monitoring data showed the maximum strain of coal is about $143.1 \mu\epsilon$, and the influence radius is about 2.0 m. When the diameter is 65 mm, and the distance is 12 mm, the maximum strain of coal is about $147.8 \mu\epsilon$, and the influence radius is about 2.6 m. When the diameter is 90 mm, and the distance is 37 mm, the maximum strain of coal is about $127.6 \mu\epsilon$, and the influence radius is about 1.6 m, as shown in Table 3 and Figure 10. Comparison of the effect before and after 5# drilling blasting is shown in Figure 11. Therefore, according to the experimental results, a drilling hole with a diameter of 65 mm and a distance of 12 mm leads to the best fracturing results, which is considered as the optimal scheme.

According to the fracturing effect enumerated in Table 3, the maximum influence radius of fracturing is 2.0 m for drilling hole with a diameter of 60 mm. According to formula (10), the blasting release energy of liquid CO₂ fracturer

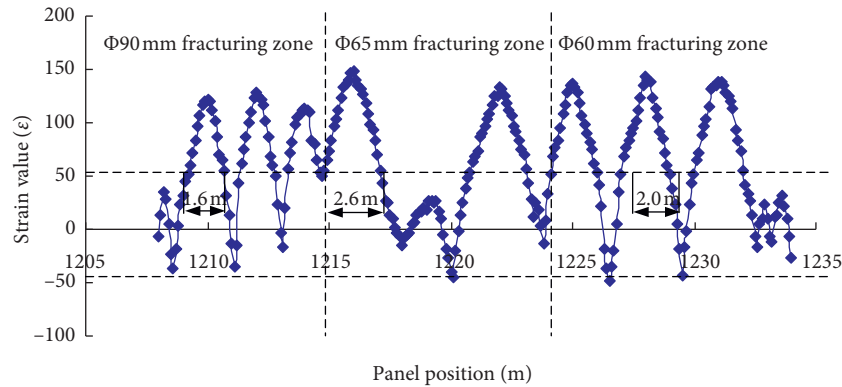


FIGURE 10: Fiber optic monitoring curve.

TABLE 3: Monitoring effect of different types of hole.

Drill number	Borehole diameter (mm)	Maximum strain value ($\mu\epsilon$)	Maximum impact area (radius) (m)
1#	60		
2#	60	143.1	2.0
3#	60		
4#	65		
5#	65	147.8	2.6
6#	65		
7#	90		
8#	90	127.6	1.6
9#	90		

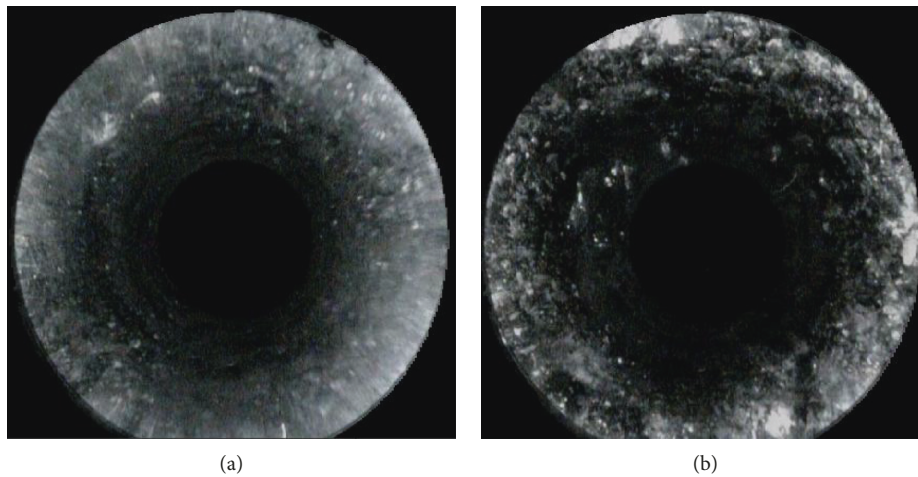


FIGURE 11: Effect diagram of 5# borehole before and after blasting: (a) before blasting, (b) after blasting.

is $6.0 \times 10^5 \text{ J} \sim 1.2 \times 10^6 \text{ J}$. According to the released energy and formula (8), the radius range of dynamic nuclear zone of dynamic system is 1.72 m~2.17 m, with an average value of 1.95 m. The difference between the measurements is 0.05 m. The maximum influence radius of fracturing is 2.6 m for drilling hole with a diameter of 65 mm. According to formula (10), the blasting release energy of liquid CO_2 fracturer is $1.31 \times 10^6 \text{ J} \sim 2.62 \times 10^6 \text{ J}$. According to the released energy and formula (8), the radius range of dynamic nuclear zone of dynamic system is 2.24 m~2.82 m, with an average value of 2.53 m. The difference between the measurements is 0.07 m.

The maximum influence radius of fracturing is 1.6 m for drilling hole with a diameter of 90 mm. According to formula (10), the blasting release energy of liquid CO_2 fracturer is $3.0 \times 10^5 \text{ J} \sim 6.1 \times 10^5 \text{ J}$. According to the released energy and formula (8), the radius range of dynamic nuclear zone of dynamic system is 1.37 m~1.73 m, with an average value of 1.55 m. The difference between the measurements is 0.05 m. Monitoring effect of different types of hole is shown in Table 4. The maximum strain value data in Table 4 used to support the findings of the radius of dynamic nuclear zone are included within the article.

TABLE 4: Monitoring effect of different types of hole.

Drill number	Maximum impact area (radius) (m)	Energy inversion results (MJ)	Calculation results of dynamic nuclear zone radius (m)	Average value of the radius (m)
1#				
2#	2.0	0.60~1.20	1.72~2.17	1.95
3#				
4#				
5#	2.6	1.31~2.62	2.24~2.82	2.53
6#				
7#				
8#	1.6	0.30~0.61	1.37~1.73	1.55
9#				

The dynamic nuclear zone radius of the dynamic system is obtained by theoretical calculation, which is subsequently compared to the measurement result. The difference between them is 0.05 m~0.07 m, and the coincidence is 96.9%~97.5%. Good consistency is achieved.

6. Conclusions

- (1) In this paper, the concept of dynamic system of coal and rock is put forward, and the relationship between dynamic system of coal and rock and rockburst appearance model is constructed. The dynamic system is divided into four regions: the dynamic nuclear zone, the damage zone, the injury zone, and the influence zone. The relationship between space structure of dynamic system and rockburst appearance is revealed. The energy source of coal and rock dynamic system is clarified.
- (2) A method for calculating the radius of dynamic nuclear zone of dynamic system is proposed, and the corresponding evaluation system is established.
- (3) The accuracy of the calculation method for the radius of dynamic nuclear zone of dynamic system is verified by the fracturing experimental data of liquid CO₂. The result shows that the degree of coincidence is 96.9%~97.5%, and good consistency is obtained. The method has high reliability and practicability and can be widely used in the rockburst prediction and risk assessment.
- (4) The liquid CO₂ fracturing method can be used to simulate the blasting source of rockburst effectively, which could be widely applied in the future.

Nomenclature

R : Radius of dynamic nuclear zone
 R_p : Radius of damage zone
 R_s : Radius of injury zone
 R_Y : Radius of influence zone
 U : The total energy of dynamic system of coal and rock
 U_Z : The energy under gravity stress field
 U_G : The energy under tectonic stress field
 U_C : The energy under mining induced stress field

γ : The density of unit bulk
 H : The depth of the location of the unit
 μ : Poisson's ratio of the unit
 E : Modulus of elasticity of the unit
 k_1 : The ratio of maximum principal stress to vertical stress
 k_2 : The ratio of intermediate principal stress to vertical stress
 k_3 : The ratio of minimum principal stress to vertical stress
 m_1 : The stress increasing coefficient of coal and rock under gravity stress field
 m_2 : The stress increasing coefficient of coal and rock under tectonic stress field
 V : The volume of dynamic nuclear zone
 R : The radius of dynamic nuclear zone
 ΔU : The released energy
 V_S : The volume of failure fractured coal
 L : The Influence radius of fracture initiation
 θ : The angle of the influence zone, random number between $[\pi/4, \pi/2]$
 U_S : The energy required for coal and rock failure
 σ_c : The uniaxial compressive strength.

Data Availability

The data used to support the findings of this study are available from the corresponding author upon request.

Conflicts of Interest

The authors declare that they have no conflicts of interest.

References

- [1] H. P. Xie, "China's coal industry must follow the path of sustainable production capacity," in *Proceedings of International Coal Summit 2013*, Beijing, China, 2013.
- [2] Y. D. Jiang, Y. S. Pan, F. X. Jiang, L. M. Dou, and Y. Jv, "State of the art review on mechanism and prevention of coal bumps in China," *Journal of China Coal Society*, vol. 29, no. 2, pp. 205–213, 2014.
- [3] L. Y. Pan, L. Q. Chen, and R. X. Zhang, "Causes for rockburst and control of gob side entry in deep two soft coal seams," *Chinese Journal of Geotechnical Engineering*, vol. 37, no. 8, pp. 1484–1489, 2015.
- [4] L. Y. Pan, R. X. Zhang, and F. P. Kong, "Study on mine pressure bumping prevention and control technology of coal mining face in seam island based on defect method," *Coal Science and Technology*, vol. 41, no. 6, pp. 14–17, 2013.
- [5] L. Y. Pan, L. J. Zhang, and X. G. Liu, *Practical Technology for Prediction and Prevention of Rock Burst*, China University of Mining and Technology Press, Xuzhou, China, 2006.
- [6] J. F. Pan, Y. Ning, D. B. Mao, H. Lan, T. T. Du, and Y. W. Peng, "Theory of rockburst start-up during coal mining," *Chinese Journal of Rock Mechanics and Engineering*, vol. 31, no. 3, pp. 586–596, 2012.
- [7] I. Vazaios, M. S. Diederichs, and N. Vlachopoulos, "Assessment of strain bursting in deep tunnelling by using the finite-discrete element method," *Journal of Rock Mechanics and Geotechnical Engineering*, vol. 11, no. 1, pp. 12–37, 2019.
- [8] C. L. Wang, X. S. Chuai, F. Shi, A. S. Gao, and T. C. Bao, "Experimental investigation of predicting rockburst using

- Bayesian model,” *Geomechanics and Engineering*, vol. 15, no. 6, pp. 1153–1160, 2018.
- [9] F. Wang and R. Kaunda, “Assessment of rockburst hazard by quantifying the consequence with plastic strain work and released energy in numerical models,” *International Journal of Mining Science and Technology*, vol. 29, no. 1, pp. 93–97, 2019.
- [10] L. R. E. Sousa, T. Miranda, R. L. E. Sousa, and J. Tinoco, “The use of data mining techniques in rockburst risk assessment,” *Engineering*, vol. 3, no. 4, pp. 552–558, 2017.
- [11] H. W. Zhang, H. Rong, J. Q. Chen et al., “Risk assessment of rockburst based on geo-dynamic division in suberect and extremely thick coal seam,” *Journal of China Coal Society*, vol. 40, no. 12, pp. 2755–2762, 2015.
- [12] Y. S. Pan, H. Luo, and Y. F. Zhao, “Application of charge induction monitoring technology of mine dynamic disasters,” *Coal Science and Technology*, vol. 41, no. 9, pp. 29–33, 2013.
- [13] Y. S. Pan, L. M. Xu, G. Z. Li, X. H. Zeng, Z. H. Li, and Y. F. Song, “Characteristics of charge radiation of dynamic disasters in deep coal mine,” *Chinese Journal of Rock Mechanics and Engineering*, vol. 33, no. 8, pp. 1619–1625, 2014.
- [14] L. M. Dou, W. Cai, S. Y. Gong, R. J. Han, and J. Liu, “Dynamic risk assessment of rock burst based on the technology of seismic computed tomography detection,” *Journal of China Coal Society*, vol. 39, no. 2, pp. 238–244, 2014.
- [15] F. X. Jiang, C. X. Shu, and C. W. Wang, “Impact risk appraisal of stope working faces based on stress superimposition,” *Chinese Journal of Rock Mechanics and Engineering*, vol. 34, no. 12, pp. 2428–2435, 2015.
- [16] J. F. Pan, Z. H. Qin, S. W. Wang, Y. X. Xia, and M. H. Feng, “Preliminary study on early warning method based on weight comprehensive and different-load sources of coal bump,” *Journal of China Coal Society*, vol. 40, pp. 2327–2335, 2015.
- [17] H. Y. Li, L. J. Kang, Z. J. Xu, Q. X. Qi, and S. K. Zhao, “Precursor information analysis on acoustic emission of coal with different outburst proneness,” *Journal of China Coal Society*, vol. 39, no. 2, pp. 384–388, 2014.
- [18] J. G. Lv, Y. D. Jiang, Y. X. Zhao, J. Zhu, and F. Gao, “Hierarchical monitoring for coal bumps and its study and application of early warning methods,” *Journal of China Coal Society*, vol. 38, no. 7, pp. 1161–1167, 2013.
- [19] Y. W. Peng, H. Lan, S. W. Wang, J. F. Pan, and Q. X. Qi, “Dynamic pre-evaluation system of bursting hazard based on geological conditions,” *Journal of China Coal Society*, vol. 35, no. 12, pp. 1997–2001, 2010.
- [20] R. F. Yuan, H. M. Li, and H. Z. Li, “Distribution of microseismic signal and discrimination of portentous information of pillar type rockburst,” *Chinese Journal of Rock Mechanics and Engineering*, vol. 31, no. 1, pp. 80–85, 2012.
- [21] J. X. Wu and J. Liu, “Calculation and application of mine microseismic positioning,” *Journal of Wuhan University of Science and Technology*, vol. 36, no. 4, pp. 308–320, 2013.
- [22] H. Rong, “Research on geodynamic conditions and dynamic system of coal and rock in wudong coal mine,” Doctor degree, Liaoning Technical University, Fuxin, China, 2016.
- [23] M. G. Qian, P. W. Shi, and J. L. Xu, *Mining Pressure and Strata Control*, China University of Mining and Technology Press, Xuzhou, China, 2010.
- [24] H. W. Zhang, H. Rong, J. Han, Z. Y. Gao, and F. Zhu, “Study on rock core discing mechanism based on stress and energy principle,” *Chinese Journal of Applied Mechanics*, vol. 31, no. 4, pp. 512–517, 2014.
- [25] W. W. Li, G. Di, and R. X. Wang, “Analysis of a liquid CO₂ tank explosion on a ship,” *Safety and Environmental Engineering*, vol. 17, no. 1, pp. 95–98, 2010.



Hindawi

Submit your manuscripts at
www.hindawi.com

